CHAPTER ONE HUNDRED SIXTY TWO

NUMERICAL SIMULATION OF SECONDARY CIRCULATION IN THE LEE OF HEADLANDS

by

Roger A. Falconer[1]
Eric Wolanski[2] and
Lida Mardapitta-Hadjipandeli[3]

ABSTRACT

The paper gives details of a study to refine and further develop a two-dimensional depth average numerical model to predict more accurately the eddy shedding features often observed in the lees of headlands. Details are given of the application of the model to Rattray Island, just east of Bowen, North Queensland, Australia, where the strong tidal currents flowing past the island give rise to separation and hydrodynamic circulation in the lee of the island.

In the governing differential equations used to predict the secondary circulation, particular emphasis has been placed on the representation of the shear stresses associated with the free shear lateral mixing layer in the downstream wake of the headland. Use of an experimentally determined lateral velocity distribution in the shear layer, together with an eddy viscosity approach, have led to the use of a relatively simple turbulence model, including both free shear layer and bed generated turbulence. A comparison of the numerically predicted velocities with corresponding field measured results around Rattray Island has shown an encouraging agreement, although there were some differences. The main difference between both sets of results was that the vorticity strength of the secondary circulation predicted in the numerical model was noticeably less than that measured in the field.

1. Lecturer in Civil Engineering, University of Birmingham, Birmingham.

2. Principal Research Scientist, Australian Institute of Marine Science, Queensland, Australia.

3. Research Student in Civil Engineering, University of Birmingham, Birmingham.

INTRODUCTION

The main objective of the research study outlined herein has been to refine and enhance a two-dimensional depth average numerical model, in an attempt to predict more accurately the tide induced eddy shedding features often observed in the lees of headlands. The model has been applied to Rattray Island, which is located just east of Bowen, North Queensland, Australia, with its geographical location being illustrated in Fig.1. This island is approximately 1.5km long, 300m wide and lies in well mixed water, having a typical depth of about 30m. Its longer axis is inclined at about 60° into the direction of the semi-diurnal tidal current, and strong tidal currents flowing past the island give rise to separation at the most northerly tip of the island and secondary circulation in the downstream lee.

A detailed field study has been undertaken by the Australian Institute of Marine Science to investigate the secondary circulation occurring around Rattray Island and to try and improve the existing knowledge of eddies shed by such headlands. In this study, outlined by Wolanski et al (1984), twenty six current meters were deployed at various sites in the south eastern lee of the island, as shown in Fig.2, with time series sea level recordings being taken around the island. Visual observations of the secondary circulation were also made using landsat imagery and aerial photography, and the surface temperature field was also measured at the time of the aerial observations. The recorded tidal ranges were generally about 3m and a strong south eastwards current was observed and measured during the rising tide. This south easterly current gave rise to a strong clockwise rotating eddy in the south eastern lee of the island. The eddy was observed to be very stable and about twice the size of the island for most of the rising tide. The surface temperature distributions and drogue trajectories also confirmed the existence of this eddy which, from measurements, was found to be several kilometres long.

The numerical model being used to simulate this eddy shedding phenomenon, for similar hydrodynamic conditions, is of the two-dimensional depth integrated type, with the water surface slope and depth mean velocity fields being evaluated from the conservation equations of mass and momentum. Included in the momentum equations are the effects of the earth's rotation, bed and surface shear forces and a simple turbulence model to represent both bed generated and free shear layer turbulence. In the numerical model, particular emphasis has been placed on: (I) formulating the lateral turbulent shear stresses in the lee of the island, (II) accurately representing the island shape and the associated boundary derivatives, (III) representing the non-linear advective accelerations so that non-linear instabilities were avoided, and (IV) investigating the influence of the Coriolis acceleration on the open boundary conditions.

GOVERNING EQUATIONS

Equations of Motions

The appropriate equations of mass and momentum conservation were derived by vertical integration of the three-dimensional continuity and Navier-Stokes equations respectively, see Falconer (1976). Thus, for the mass conservation equation in the horizontal plane, integration yields:-

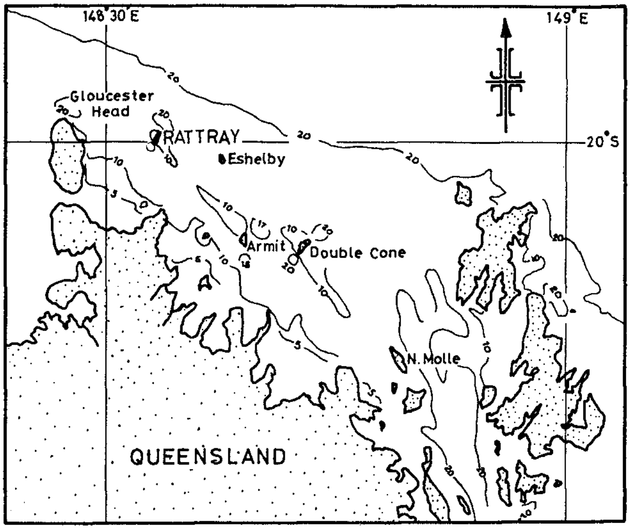

Fig.1 Location of Rattray Island and bathymetry (in fathoms)

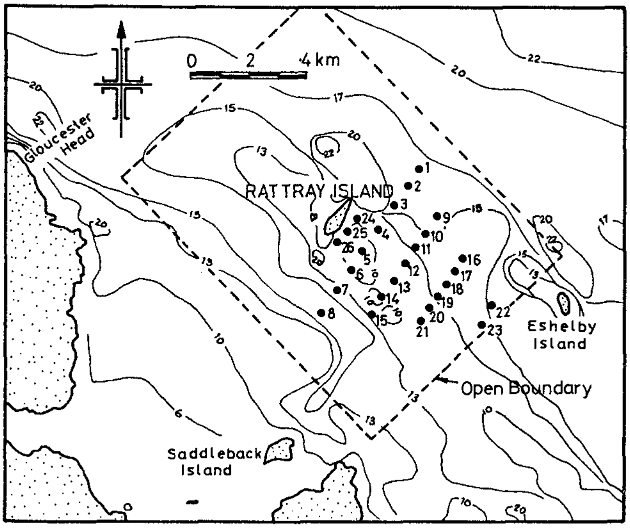

Fig.2 Area around Rattray Island showing location of current meters and model boundary

$$\frac{\partial \eta}{\partial t} + \frac{\partial UH}{\partial x} + \frac{\partial VH}{\partial y} = 0 \qquad \ldots\ldots\ (1)$$

where η = water surface elevation above mean sea level, U, V = depth average velocity components in the x, y co-ordinate directions respectively, and H = total depth of flow.

Likewise, for an incompressible turbulent fluid flow on a rotating earth, the depth integrated equations for horizontal momentum in the x and y directions respectively, can be written as:-

$$\frac{\partial UH}{\partial t} + \beta\left[\frac{\partial U^2 H}{\partial x} + \frac{\partial UVH}{\partial y}\right] - fVH + gH\frac{\partial \eta}{\partial x} - \frac{\tau_{wx}}{\rho} + \frac{\tau_{bx}}{\rho}$$

$$- \frac{1}{\rho}\left[\frac{\partial H\sigma_{xx}}{\partial x} + \frac{\partial H\tau_{xy}}{\partial y}\right] = 0 \qquad \ldots\ldots\ (2)$$

$$\frac{\partial VH}{\partial t} + \beta\left[\frac{\partial UVH}{\partial x} + \frac{\partial V^2 H}{\partial y}\right] + fUH + gH\frac{\partial \eta}{\partial y} - \frac{\tau_{wy}}{\rho} + \frac{\tau_{by}}{\rho}$$

$$- \frac{1}{\rho}\left[\frac{\partial H\tau_{yx}}{\partial x} + \frac{\partial H\sigma_{yy}}{\partial y}\right] = 0 \qquad \ldots\ldots\ (3)$$

where β = correction factor for non-uniformity of the vertical velocity profile (assumed to be 1.016 for a seventh power law velocity distribution), f = Coriolis parameter, g = gravitational acceleration, ρ = fluid density, τ_{wx}, τ_{wy} = surface shear stress components due to wind action, τ_{bx}, τ_{by} = bottom shear stress components due to bed friction, and σ_{xx}, τ_{xy}, τ_{yx}, σ_{yy} = Reynolds stress components in the x,y directions respectively.

In the present study the effects of wind action have not been considered, and hence τ_{wx} and τ_{wy} have both been equated to zero. For the bottom stresses, the terms have been represented in a quadratic form (see Dronkers(1964)) giving:-

$$\left.\begin{aligned} \tau_{bx} &= \frac{\rho g U\sqrt{U^2+V^2}}{C^2} \\ \tau_{by} &= \frac{\rho g V\sqrt{U^2+V^2}}{C^2} \end{aligned}\right\} \qquad \ldots\ldots\ (4)$$

where C = Chezy roughness coefficient (defined by $H^{1/6}/n$, where n is the Manning roughness coefficient).

In the modelling of turbulent flows, particularly where secondary circulation and notable lateral velocity gradients exist, the direct shear stresses σ_{xx} and σ_{yy} are generally small in comparison with the lateral shear stresses τ_{xy} and τ_{yx}, see Kuipers and Vreugdenhil(1973).

Since this condition appeared to apply in this study, the direct stress components σ_{xx} and σ_{yy} have been neglected from the momentum equations (2) and (3) respectively. However, the significance and importance of the lateral shear stresses is not obvious in any study involving recirculating flows, and hence an analysis of the vorticity transport equation - corresponding to the momentum equations (2) and (3) - has been undertaken in an attempt to indicate the importance of these terms.

Vorticity Transport Equation

In order to obtain the appropriate depth mean vorticity transport equation from the momentum equations (2) and (3), the wind stresses and direct stresses were neglected and the momentum correction factor β was assumed to be unity for simplicity. Hence, differentiation of Eqs. (2) and (3) with respect to y and x respectively, and subtraction of the corresponding equations gives:-

$$\underbrace{\frac{\partial\omega}{\partial t}}_{(1)} + \underbrace{U\frac{\partial\omega}{\partial x} + V\frac{\partial\omega}{\partial y}}_{(2)} + \underbrace{(\omega - f)\left[\frac{\partial U}{\partial x} + \frac{\partial V}{\partial y}\right]}_{(3)} + \underbrace{\left[\frac{\partial}{\partial y}\left(\frac{\tau_{bx}}{\rho H}\right) - \frac{\partial}{\partial x}\left(\frac{\tau_{by}}{\rho H}\right)\right]}_{(4)}$$

$$\underbrace{- \frac{\partial}{\partial y}\left[\frac{1}{\rho H}\frac{\partial H\tau_{xy}}{\partial y}\right] + \frac{\partial}{\partial x}\left[\frac{1}{\rho H}\frac{\partial H\tau_{yx}}{\partial x}\right]}_{(5)} = 0 \quad \ldots\ldots (5)$$

where ω = depth mean vorticity = $\left(\frac{\partial U}{\partial y} - \frac{\partial V}{\partial x}\right)$

The various terms of Eq.(5) refer to:- (1) the time rate of change of vorticity, (2) advection of vorticity, (3) convergence or divergence of vorticity by the mean flow, (4) effects of bottom friction, and (5) moments of the lateral stresses about a vertical axis.

If a conventional control volume approach is adopted in analysing this equation, it can be shown that the generation of vorticity (or secondary circulation) is only affected by terms (3), (4) and (5) - see Flokstra (1977). Furthermore, the bottom friction term (4) can be shown to have a negative generation effect, i.e. it tends to dissipate any vorticity generated. Such an analysis therefore indicates that secondary circulation (or vorticity) in the lee of a headland, for example, can only be generated by:- (i) the advective terms (3), and (ii) the lateral shear stresses (5). Hence, in this study the representation and inclusion of the lateral shear stresses in the mathematical model is of considerable importance if secondary circulation is to be modelled with any degree of accuracy. In addition to the importance of the lateral shear stresses in recirculating flows, Kuipers and Vreugdenhil (1973) and Flokstra (1977) have shown that the use of a no-slip boundary condition at all solid boundaries is also important in generating vorticity in such flow fields.

Formulation of Lateral Shear Stresses.

Having established the importance of the lateral shear stresses in modelling secondary circulation, consideration was then given to formulating these terms as accurately as possible without the use of a multi-equation turbulence model, such as the k-ε model. The disadvantages of using such refined turbulence models for tide induced secondary circulation are that:- (i) there is a lack of adequate tidal flow data for the empirical constants included in such models, and (ii) there is a significant increase in the computational effort required.

In adopting a simpler approach to the formulation of the lateral shear stresses, the turbulence in the mixing zone in the lee of the headland was first separated into its two components, namely:- (i) bed generated turbulence, and (ii) free shear generated turbulence arising between the main flow and the eddy as a result of relatively large horizontal velocity gradients. However, in the mixing region immediately downstream of the headland, free shear layer generated turbulence tends to dominate over bed generated turbulence and hence more emphasis has to be placed on this component.

In establishing a formulation for the free shear layer turbulence component, use has been made of some of the semi-empirical concepts and approaches developed from extensive experimental studies of the velocity field characteristics in wakes and jet flows. These investigations have been undertaken by a number of authors and are reviewed in Townsend (1956).

The pronounced horizontal velocity gradients occurring in the mixing region downstream of the headland have been approximated in the evaluation of the free shear layer stress components by assuming an observed universal velocity profile of the form given by Townsend(1956). Using the notation illustrated in Fig.3, this velocity profile can be simplified as outlined by Lean and Weare (1979) to give:-

$$U = \frac{U_1}{2}\left\{1 + \text{erf}\left[\frac{y}{x}\left(\frac{Rs}{2}\right)^{\frac{1}{2}}\right]\right\} \qquad \ldots\ldots (6)$$

where U_1 = free stream velocity and Rs = experimental constant ≅ 288. In adopting an eddy viscosity approach, together with a Boussinesq representation of the shear stresses, observations suggest that a mean eddy viscosity can be applied across the shear layer, see Townsend (1956). In applying this approximation in the mixing layer, the resulting eddy viscosity can be shown to be of the following form:-

$$\varepsilon_\ell \cong \frac{U_1 x}{2Rs} \qquad \ldots\ldots (7)$$

where ε_ℓ = mean eddy viscosity across the mixing layer, and with the rate of spread of the mixing layer being assumed to be constant. In turn, it can be shown that the eddy viscosity, the length scale of turbulence and the width of the shear layer are all linearly dependent upon the longitudinal distance and independent of the lateral distance. Furthermore, although the eddy viscosity increases linearly with x, the maximum shear stress (τ_{xy} at $y = 0$) remains constant since the lateral

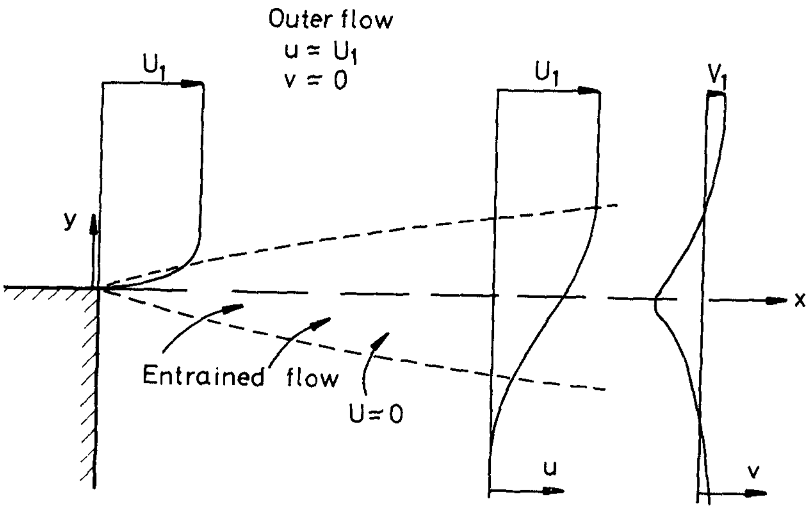

FIG.3 Typical velocity profile occurring in the mixing zone downstream of a headland.

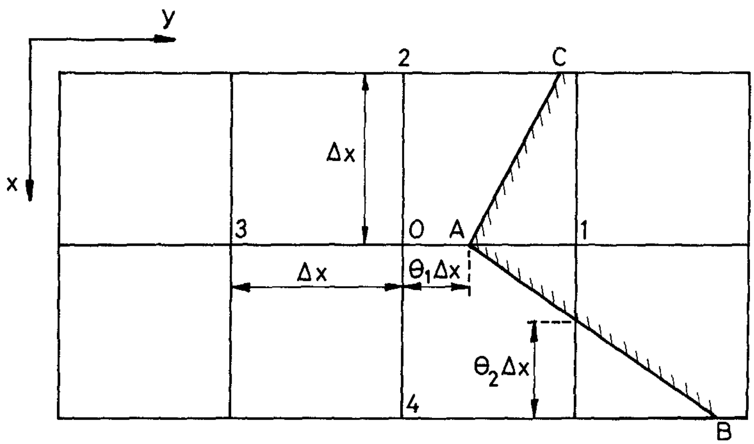

FIG.4 Non-uniform grid spacing around headland for more accurate boundary representation.

velocity gradient $\frac{\partial U}{\partial y}$ decreases linearly with x (see Lean and Weare (1979)) that is:-

$$\tau_{xy_{max}} = \rho\varepsilon_{\ell}\frac{\partial U}{\partial y} = \rho\frac{U_1^2}{2}\frac{1}{\sqrt{2\pi Rs}} \cong 0.012\rho U_1^2 \quad .... \ (8)$$

For the bed generated component of turbulence, the vertical velocity profile can be approximated to a logarithmic form - for the purpose of closure of the momentum equations - with the result that the spatially varying eddy viscosity follows the well documented form, as reviewed by Fischer (1973):-

$$\varepsilon_b \cong 0.16U_*H \quad ...... \ (9)$$

where ε_b = bed generated eddy viscosity and U_* = shear velocity = $\sqrt{g}U_s/C$ - where Us is the fluid speed.

In comparing the rate of production of turbulence in the mixing layer with that of the bed, Lean and Weare (1979) have shown that the bed generated turbulence becomes re-established in the mixing layer[2] when:-

$$\frac{x}{H} > \frac{2}{\pi}\frac{C^2}{g} \quad ...... \ (10)$$

Hence, combining both free shear layer and bed generated turbulence in the momentum equations, the resulting lateral shear stress representation used in the mathematical model can be summarised as follows:-

$$\tau_{xy} = \rho\varepsilon\frac{\partial U}{\partial y} = \rho\left\{\frac{U_1x}{2Rs} + \frac{0.16\sqrt{g}Us}{C}\right\}\frac{\partial U}{\partial y} \quad ...... \ (11)$$

with the shear stress beyond the mixing layer, i.e. $x > 2C^2H/(\pi g)$, being defined simply by bed generated turbulence as:-

$$\tau_{xy} = \rho\left[\frac{0.16\sqrt{g}Us}{C}\right]\frac{\partial U}{\partial y} \quad ...... \ (12)$$

The boundaries of the mixing layer in the lateral plane were obtained from equation (6), which was assumed to apply within the limits:-

$$0.05\,U_1 < U < 0.95\,U_1 \quad ...... \ (13)$$

and with shear generated turbulence again being equated to zero outside these bounds.

NUMERICAL SPECIFICATIONS

Finite Difference Representations

The finite difference equations corresponding to the governing differential equations were expressed in an alternating direction implicit form, with all terms being fully centred in time and space - except for the second derivatives of the velocity components immediately adjacent to the island boundary. The non-linear advective accelerations and the second derivatives associated with the lateral shear stresses were time centred by iteration. The second order scheme, with accuracy $0(\Delta t^2, \Delta x^2)$, involved discrete values of the variables being represented using a space staggered grid scheme, in which water elevations and velocity components were described at different grid locations.

The only terms requiring special mention are the advective accelerations expressing the lateral transport of momentum in the x and y directions of the momentum equations, i.e. the UV product components of the advective accelerations in equations (2) and (3). These terms were represented in the finite difference scheme using the marker and cell technique, in that the spatial location of the velocity component in the direction of motion under consideration was governed by the direction of the perpendicular velocity component, see Williams and Holmes (1974). This representation was similar to that of upwind differencing and had the advantage that:- (i) the corresponding momentum flux was evaluated nearer to the position where it originated and (ii) no grid scale oscillations were apparent since this scheme included sufficient damping to counteract the occurrence of such oscillations.

In view of the significance of the headland shape on the characteristics of the downstream velocity field, the finite difference representation was refined immediately adjacent to the headland so that the island geometry could be represented as accurately as possible. Hence, instead of using a uniform grid space representation across the whole computational field, the first and second derivatives were adjusted, where necessary, within the grid squares around the headland so that the actual boundary location was defined in the model. An example of the boundary representation for the headland is illustrated in Fig.4, with the corresponding first and second derivatives in the y direction at point O being defined as (see Smith (1978)):-

$$\left.\frac{\partial U}{\partial y}\right|_o = \frac{1}{\Delta x}\left[\frac{1}{\theta_1(1+\theta_1)}U_A - \frac{(1-\theta_1)}{\theta_1}U_o - \frac{\theta_1}{(1+\theta_1)}U_3\right] \quad \ldots\ldots \quad (14)$$

$$\left.\frac{\partial^2 U}{\partial y^2}\right|_o = \frac{1}{\Delta x^2}\left[\frac{2}{\theta_1(1+\theta_1)}U_A + \frac{2}{(1+\theta_1)}U_3 - \frac{2U_o}{\theta_1}\right] \quad \ldots\ldots \quad (15)$$

where the subscripts refer to the notation given in Fig.4. The resulting equations have leading errors of $0(\Delta x^2)$ and $0(\Delta x)$ respectively, and can be simplified for a no-slip boundary requirement since $U_A = 0$ for the example given. Tests were undertaken on the application and comparability of this scheme with a regular grid representation for a one-dimensional flat bottomed estuary having similar dimensions and hydrodynamic boundary conditions as for the present study. The numerically predicted water elevations and velocities at the estuary head agreed to within a few percent for the irregular and regular grids, and compared favourably with the analytical results for linear waves (see Ippen (1966)) and the semi-analytical results for non-linear waves (see Proudman (1957)) - which included the effects of the advective accelerations and bottom friction. Hence, no marked numerical diffusion was expected to occur near the headland as a result of using such a representation, and non-linear instabilities were not encountered in any of the subsequent simulations incorporating Eqs. (14) and (15) and similar representations for the other derivatives.

For the model simulations a mesh of 40 x 29 grid squares was used, with a grid spacing (Δx) of 300m. At the centre of each grid square a representative depth between mean sea level and the bed was required, with the corresponding data being obtained from bathymetric charts provided by the Australian Institute of Marine Science. The resulting bathymetry used in the mathematical model can be seen in the isoparametric projection illustrated in Fig.5. Since no data was available concerning the characteristics of the bed roughness, all of the mathematical simulations were undertaken for an assumed Manning roughness coefficient of 0.025. This value of n appeared to be a reasonable choice based on Knight's (1981) measurements in the Conwy Estuary, where similar tidal ranges are experienced.

Open Boundary Conditions

The boundary conditions for the hydrodynamic model were taken from field measured water elevations and velocities recorded over a period of four tides. At the northernmost boundary water elevations were defined at 10 minute intervals using data recorded around the island perimeter, together with the inclusion of an approximate phase lag of $L\sqrt{gH}$ - where L is the distance from the boundary to the island. Two representations of the lateral surface slope were considered in the simulations including:- (i) a horizontal water surface slope with $\eta = f(t)$ only, or $\partial\eta/\partial y = 0$, and (ii) a surface slope governed by the Coriolis acceleration with $\eta = f(y,t)$. In both simulations the lateral velocity component along the boundary (V) was assumed to be zero, which resulted in the latter and more accurate boundary representation being governed by the resulting form of the momentum equation (3), i.e.:-

$$\frac{\partial\eta}{\partial y} = -\frac{fU}{g} \qquad \ldots\ldots \quad (16)$$

On comparing the two simulations, the use of a horizontal surface slope gave unrealistic velocity field predictions, whereas from a purely observational viewpoint the second representation, i.e. Eq.(16), appeared to give realistic results.

At the western and eastern boundaries a free slip wall was assumed to exist, with only the lateral velocity component (V) therefore being zero along the boundary walls. Finally, at the southernmost boundary velocities were defined, again at 10 minute intervals, from field measurements taken at site number 23, which was located as shown in Fig.2. The velocity along this boundary was assumed to be uni-directional, with the result that U = f(t) only and V = O.

The open boundary water elevations and velocities required at every half timestep of 60 seconds were obtained by quadratic interpolation from the field data. The model simulations were always started from rest, i.e. U = V = 0 everywhere, with the initial mean water elevation across the computational domain being coincident with the

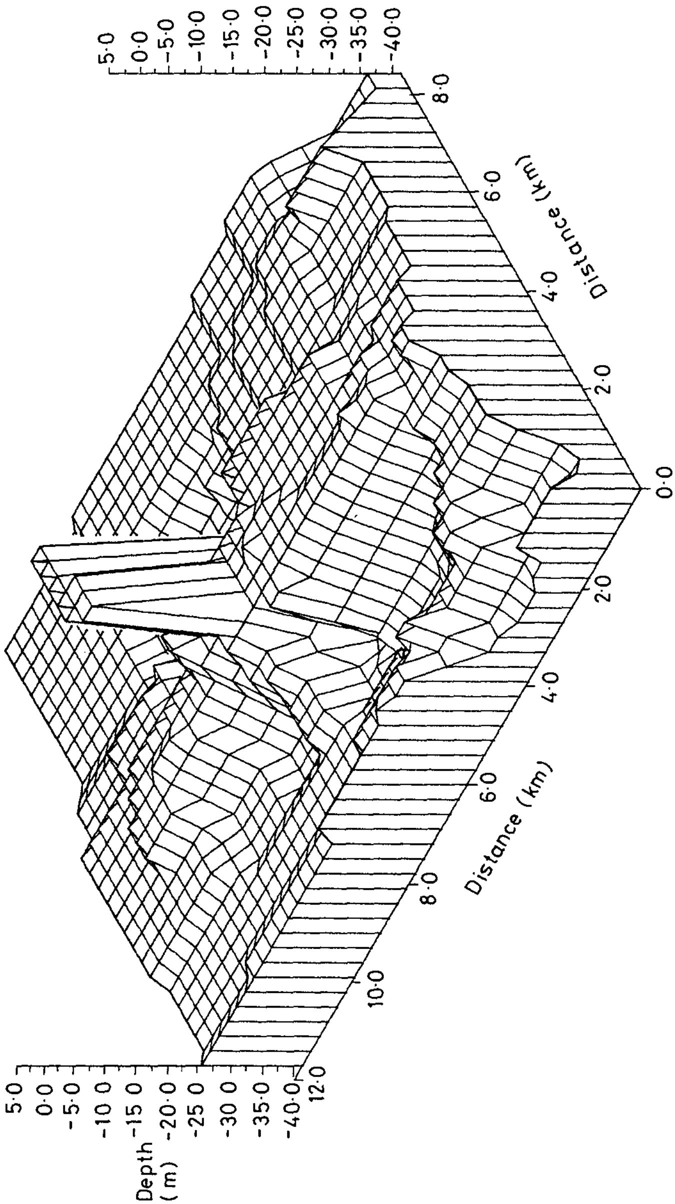

Fig.5 Three-dimensional representation of the bathymetry around Rattray Island

elevation closest to the zero velocity condition obtained from field data.

NUMERICAL MODEL RESULTS

Although this study forms part of an on-going research programme on numerical modelling of secondary circulation around headlands, a number of model simulations have been undertaken to date which have allowed comparisons to be made with the field measurements and observations. In all of these simulations the same water elevation and velocity variations were applied at the open boundaries, with the model being run for up to 50 hours, i.e. almost four tides.

In the first of these simulations direct comparisons have been made between the field measured velocities at the current meter positions shown in Fig.2, and the numerically predicted velocities at the grid points closest to these meter positions. Synoptic current meter measurements at three different tidal phases are shown in Fig.6, with the corresponding numerical model predictions for the optimum island geometry being given in Fig.7. When the corresponding results of Figs. 6 and 7 are compared, it can be seen that the overall agreement between the predicted and the measured velocities and field observations is reasonably encouraging, with some distinct similarities. Firstly, the occurrence of the eddy in the lee of the island was first identified some 2 hours into the flood tide. This compared reasonably well with current measurements, in that Wolanski et al (1984) found that the current direction close to and in the lee of the island started to rotate clockwise after one hour into the flood tide. Further similarities between both sets of results were in the dimensions of the eddy, in that predictions and observations indicated that the eddy size was about the same width as the island and that the maximum length of the eddy was about twice the island width.

However, apart from these similarities, there were some important differences between both sets of results, with some of these differences forming the basis of current research in this field by the authors. The main difference between both sets of results was that the vortex strength of the eddy was noticeably less in the numerical model predictions. This was chiefly thought to be due to:- (i) the coarseness of the grid, which is presently being refined for future studies, and (ii) the reduction in size of the lateral shear stress gradient in the model as a consequence of using a finite difference representation for the velocity gradient in the mixing zone, i.e. Eq. (11) within the limits defined by Eq.(13), rather than the semi-empirical velocity gradient defined by Eq.(6). Secondly, the entrainment of the jet flow just downstream of the island tip, along the separation streamline, was found to be less marked in the numerical model - with this discrepancy also thought to be due to the previously mentioned inaccuracies. Finally, the centre of rotation of the eddy in the numerical model predictions was always observed to be too far west of the corresponding field measured and observed eddy centre. This discrepancy was thought to be due to inadequate consideration being given in the model to the flow conditions at the diametrically opposite island tip, where the influence of the separation phenomena on the downstream velocity field was known to be less pronounced.

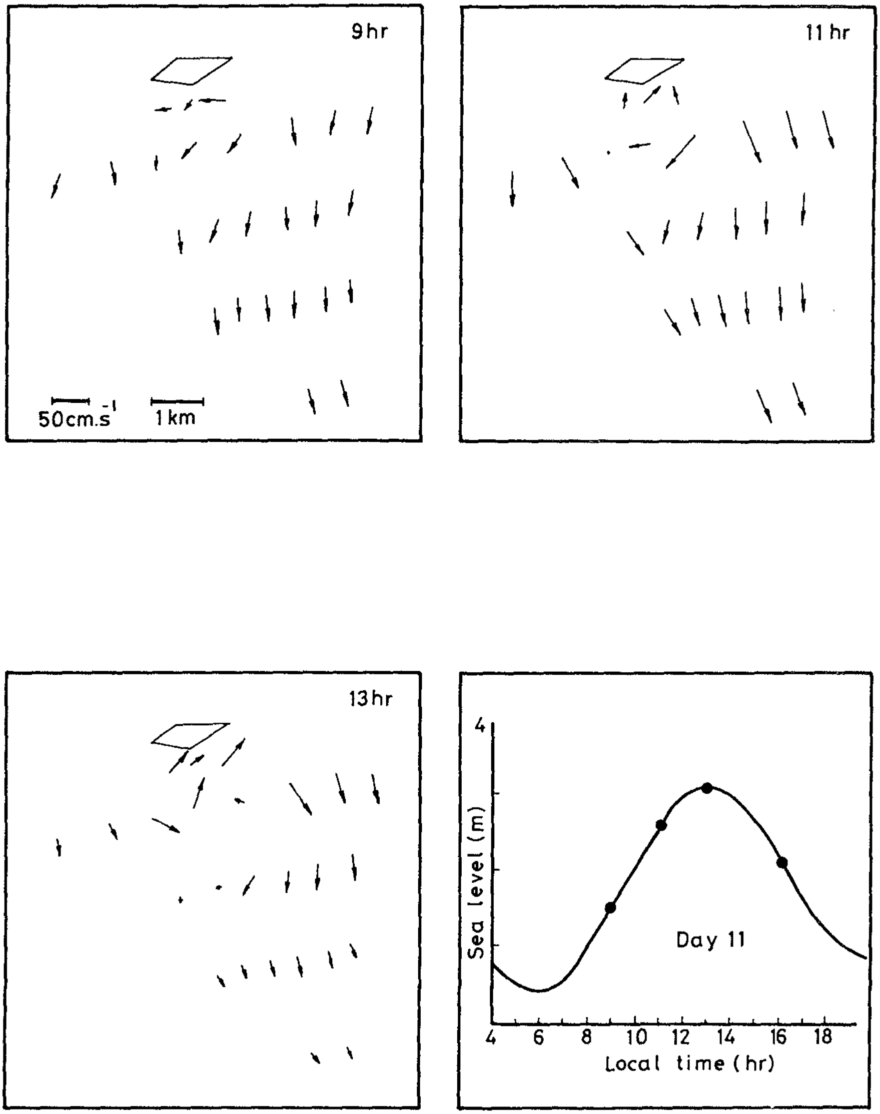

Fig.6 Field measured velocities at the measuring sites

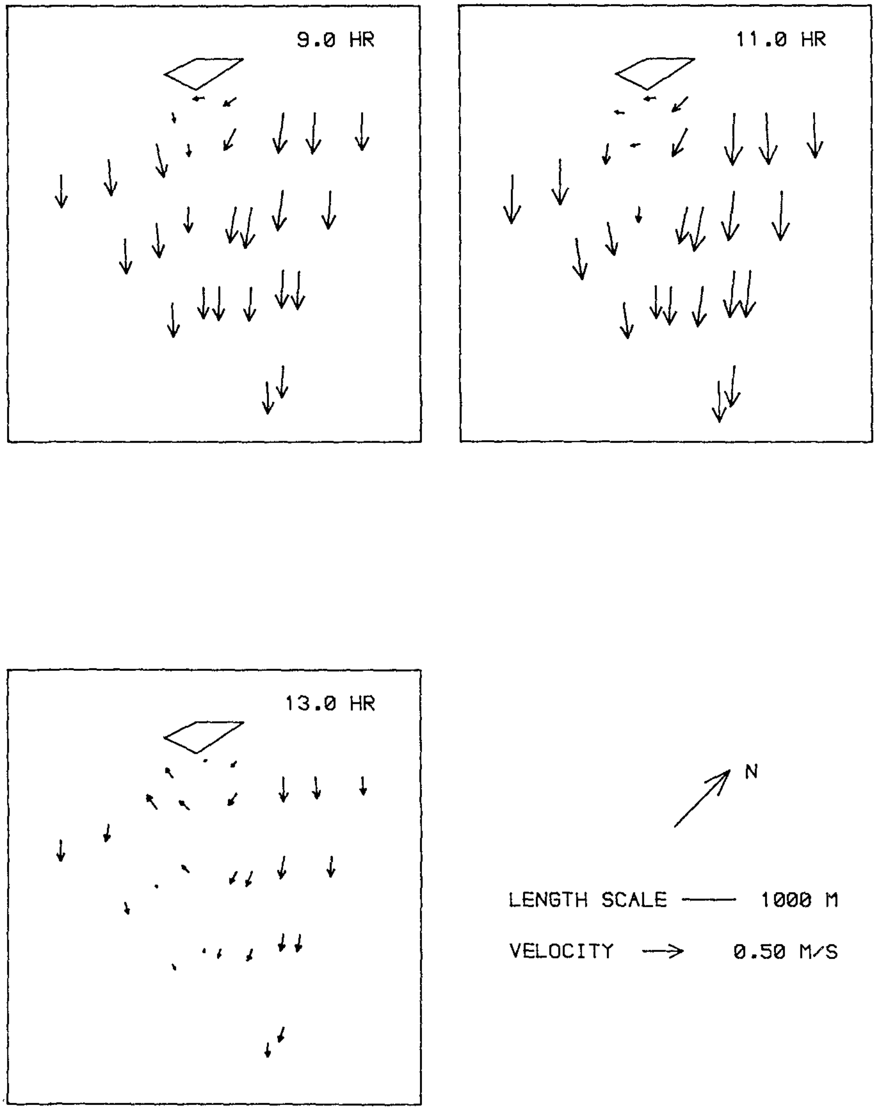

Fig.7 Numerically predicted velocities near the measuring sites using a non-uniform grid around the island

Further similar tests and comparisons were undertaken for different grid representations of the island geometry, see Mardapitta-Hadjipandeli (1984). These tests included the adoption of:- (i) a regular square mesh, and (ii) impermeable thin plate walls for the island, although detailed comparisons with the results for the irregular mesh shown in Fig.7 indicated that the latter gave the closest similarity to the field measured results.

A series of tests were also undertaken to investigate the influence of the various terms of the equations of motion on the secondary circulation characteristics. These results were compared with the velocity field prediction for the whole computational field at 13.3 hours after the start of simulation, i.e. just after high tide, with the corresponding prediction being illustrated in Fig.8.

Although no field measurements have been taken in the northern lee of the island, comparisons were also made with the velocity field predictions at 18.5 hours, where the mathematical model results showed the existence of two well defined counter rotating eddies in the region, see Fig.9. The main results of this series of tests showed that no eddies occurred in either lee of the island when the advective accelerations and the lateral shear stresses were excluded from the model, see Fig.10, and that inclusion of the Coriolis term at the open boundary was essential for realistic velocity field predictions, see Mardapitta-Hadjipandeli (1984).

CONCLUSIONS

As part of an on-going research programme to develop a reliable mathematical model of secondary circulation in the lee of headlands, such a mathematical model is being developed and refined to predict the tide induced eddies, observed and measured in the field, around Rattray Island. The model includes a relatively simple zero-equation turbulence model, with particular emphasis being placed on the modelling of the free shear layer turbulence occurring in the mixing zone along the separation streamline - formed at the separation point at the island's most easterly tip. This component of the turbulence structure has been included in the model using an eddy viscosity approach, and a universal lateral velocity distribution, which is based on extensive field and experimental measurements for velocity fields in jet flows and wakes.

The numerical model predictions to-date have been compared with extensive field measurements and, although the agreement between both sets of results is reasonably encouraging, there are some important differences. These differences include:- (i) a weaker vortex strength, (ii) less entrainment into the mixing zone, and (iii) a difference in location of the centre of rotation of the eddy between the field measured and the numerically predicted results.

In addition to these comparisons, further tests have been undertaken to investigate the hydrodynamic phenomena being modelled. These tests showed that:- (i) exclusion of the Coriolis acceleration along the water level boundary gave unrealistic results, (ii) use of an irregular grid adjacent to the island gave improved results, with

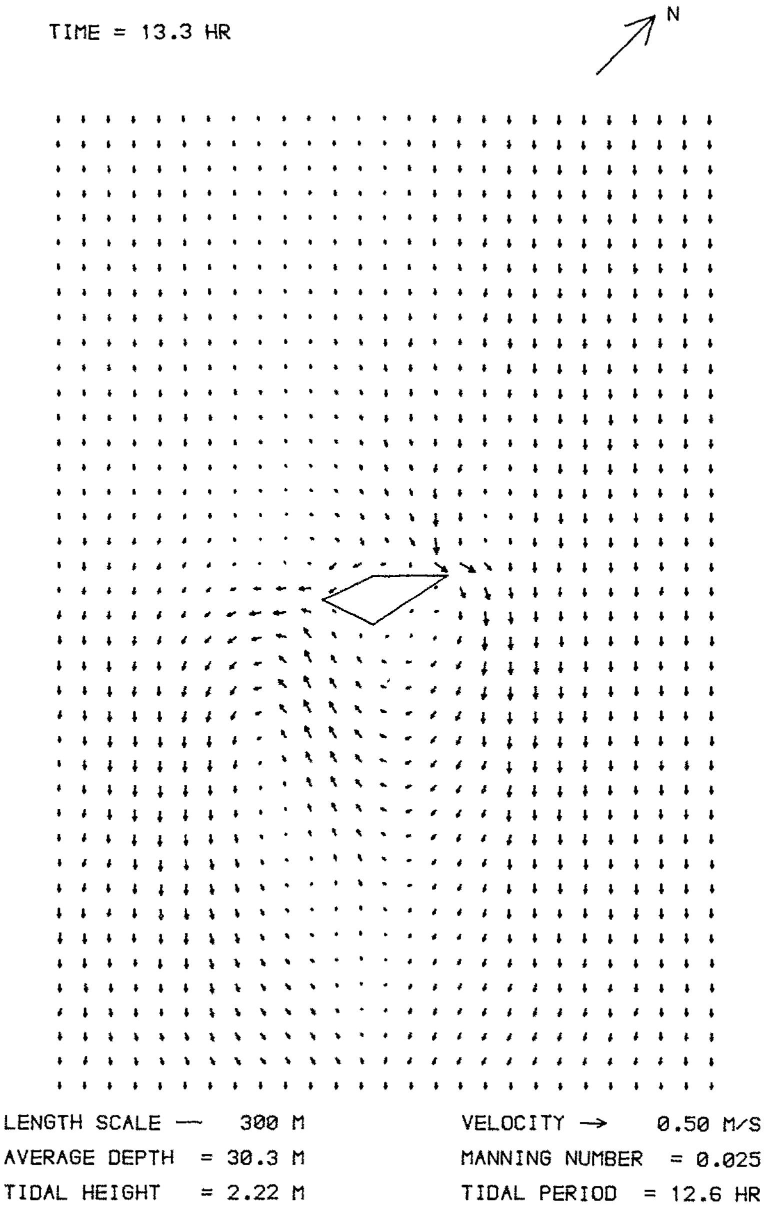

Fig.8 Numerically predicted velocities around Rattray Island at High Water Level

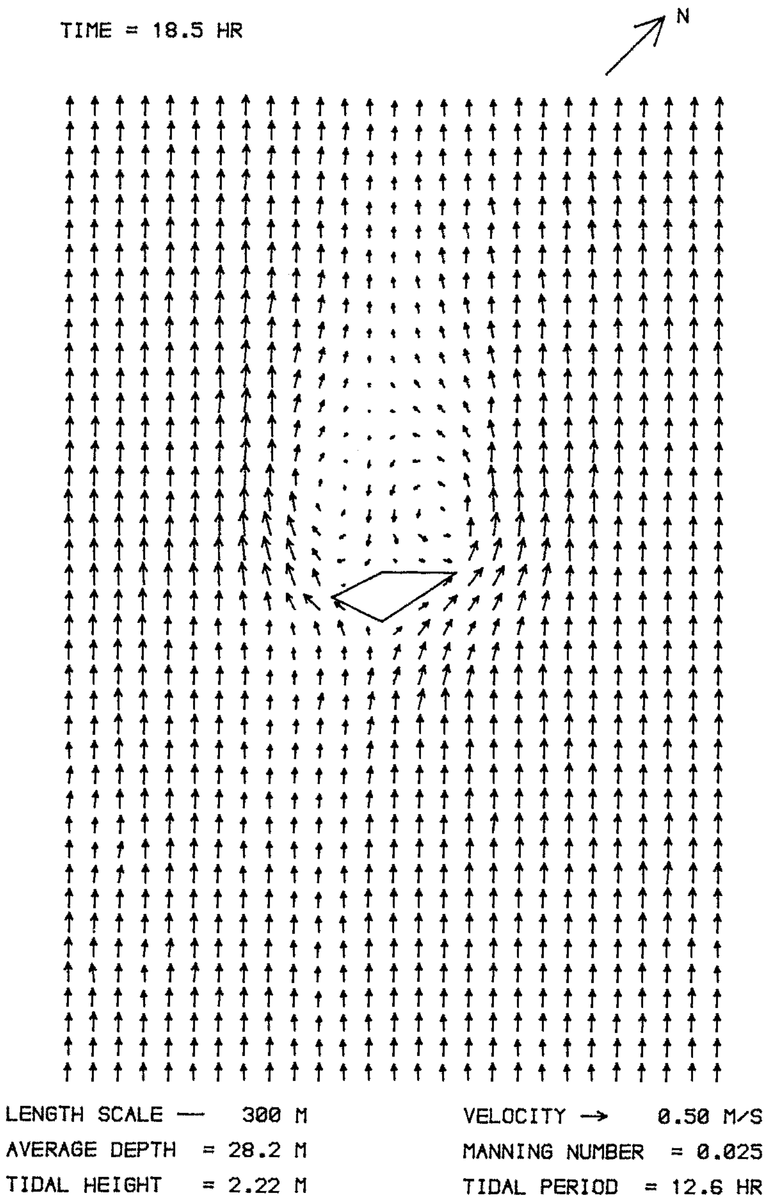

Fig.9 Numerically predicted velocities around Rattray Island near low water level during ebb tide.

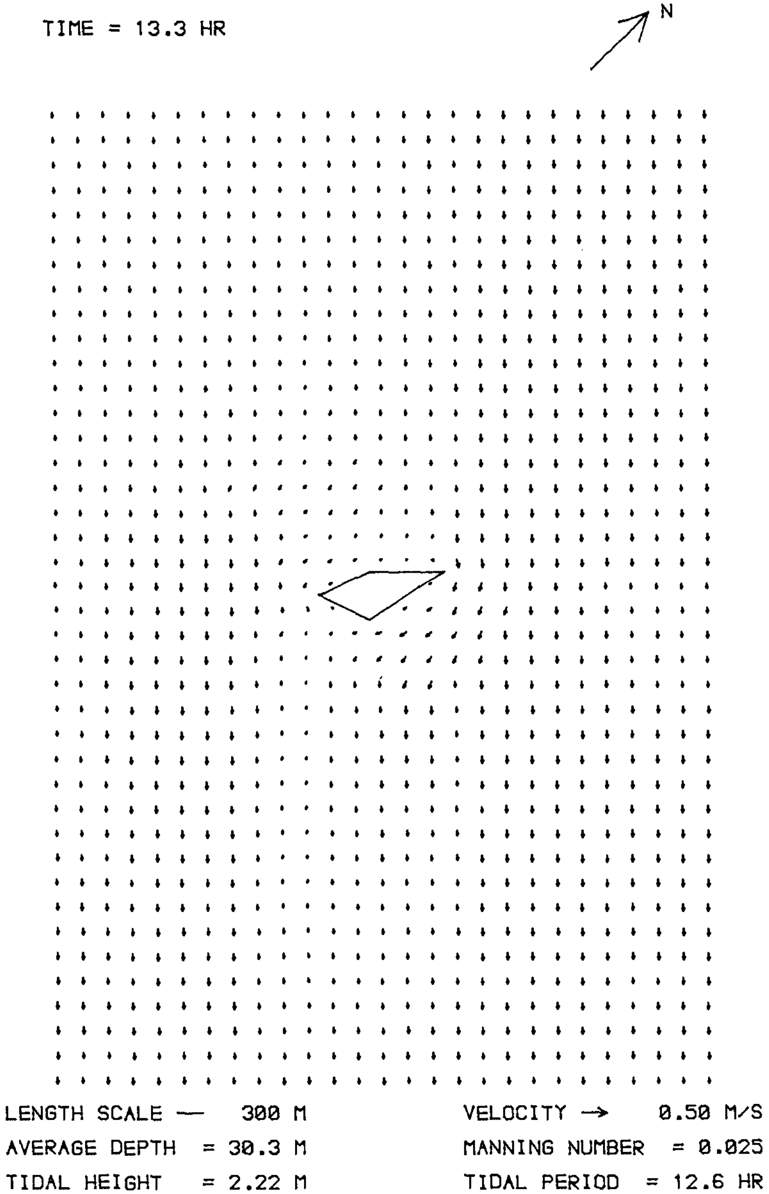

Fig.10 Numerically predicted velocities around Rattray Island at high water level excluding the advective accelerations

no indications of marked numerical diffusion, and (iii) no secondary circulation was predicted in the model when the advective accelerations and the lateral shear stresses were excluded. The latter conclusion from these tests confirmed the results of an analysis of the vorticity transport equation, where it was shown that the only terms generating vorticity in the model were the advective accelerations and the lateral shear stresses.

ACKNOWLEDGEMENTS

The model developments were undertaken at the Department of Civil Engineering, of the University of Birmingham, with the study being partially funded by a Science and Engineering Research Council research studentship.

This study in its present form would not have been possible without the use of extensive field data being made available by the Australian Institute of Marine Science, Queensland, Australia.

REFERENCES

1. DRONKERS, J.J. (1964). "Tidal Computations in Rivers and Coastal Seas". North Holland Publishing Company, Amsterdam.
2. FALCONER, R.A. (1976). "Mathematical Modelling of Jet-Forced Circulation in Reservoirs and Harbours". Ph.D. Thesis, University of London, England, 237pp (unpublished)
3. FISCHER, H.B. (1973). "Longitudinal Dispersion and Turbulent Mixing in Open Channel Flow". Annual Review of Fluid Mechanics, Vol.5, pp.59-78.
4. FLOKSTRA, C. (1977). "The Closure Problem for Depth-Averaged Two-Dimensional Flow". Paper A106, 17th International Association for Hydraulic Research Congress, Baden-Baden, Germany, pp.247-256.
5. IPPEN, A.T. (Ed.) (1966). "Estuary and Coastline Hydrodynamics". Engineering Society Monographs, McGraw-Hill Book Company Inc., New York.
6. KNIGHT, D.W. (1981). "Some Field Measurements Concerned with the Behaviour of Resistance Coefficients in a Tidal Channel". Estuarine, Coastal and Shelf Science, Vol.12, pp.303-322.
7. KUIPERS, J. and VREUGDENHIL, C.B. (1973). "Calculations of Two-Dimensional Horizontal Flow". Report No.S163, Part 1, Delft Hydraulics Laboratory, Delft, October.
8. LEAN, G.H. and WEARE, T.J. (1979). "Modelling Two-Dimensional Circulating Flow". Journal of the Hydraulics Division, ASCE, Vol.105, No.HY1, January, pp.17-26.
9. MARDAPITTA-HADJIPANDELI, L. (1984). "The Numerical Modelling of Tide-Induced Circulation." M.Sc. (Qual.) Thesis, University of Birmingham England, 155pp (unpublished).
10. PROUDMAN, J. (1957). "Oscillations of Tide and Surge in an Estuary of Finite Length". Journal of Fluid Mechanics, Vol.2, pp.371-382.
11. SMITH, G.D. (1978). "Numerical Solution of Partial Differential Equations". Oxford University Press, Second Edition.
12. TOWNSEND, A.A. (1956). "The Structure of Turbulent Shear Flow". Cambridge University Press, Cambridge, England.

13. WILLIAMS, J.W. and HOLMES, D.W.(1974). "Marker-and-Cell Technique, a Computed Programme for Transient Stratified Flows with Free Surfaces". Report No.134, Hydraulics Research Station, Wallingford pp.54.
14. WOLANSKI, E., IMBERGER, J. and HERON, M.(1984). "Island Wakes in Shallow Coastal Waters". Journal of Geophysical Research(in Press).

NOTATION

C	= Chezy roughness coefficient
f	= Coriolis parameter
g	= gravitational acceleration
H	= total depth of flow
L	= distance from open boundary to island
n	= Manning roughness coefficient
Rs	= experimental constant
t	= time
U,V	= depth averaged velocity components in the x,y directions
U_1	= free stream velocity
U_*	= shear velocity
U_S	= fluid speed
x,y	= mutually perpendicular co-ordinate axes in the horizontal plane
β	= correction factor for non-uniformity of the vertical velocity profile
Δt	= time step
Δx	= grid spacing
ε_b	= eddy viscosity due to bed generated turbulence
ε_ℓ	= eddy viscosity due to free shear layer generated turbulence
η	= water surface elevation above mean sea level
ρ	= fluid density
σ_{xx},σ_{yy}	= direct stress components in the x,y directions
τ_{xy},τ_{yx}	= lateral shear stress components in the x,y directions
τ_{bx},τ_{by}	= bed shear stress components in the x,y directions
τ_{wx},τ_{wy}	= wind induced surface shear stress components in the x,y directions
ω	= depth average vorticity about the vertical axis